Inorganica Chimica Acta 362 (2009) 3225–3230

Contents lists available at ScienceDirect

Inorganica Chimica Acta

journal homepage: www.elsevier.com/locate/ica

Silver(I) methanesulfonate complexes containing diphosphine ligands: Spectroscopic and structural characterization

Claudio Pettinari [a,*], Jean Ngoune [a], Alessandro Marinelli [a], Brian W. Skelton [b], Allan H. White [b]

[a] *Dipartimento di Scienze Chimiche, Università di Camerino, via S. Agostino 1, 62032 Camerino (MC), Italy*
[b] *Chemistry M313, SBBCS, University of Western Australia, Crawley, WA 6009, United States*

ARTICLE INFO

Article history:
Received 10 December 2008
Received in revised form 22 February 2009
Accepted 23 February 2009
Available online 9 March 2009

Keywords:
Ag(I) complexes
Diphosphine ligands
Crystal structure
Spectroscopy

ABSTRACT

1:1 and 2:1 adducts of diphosphine ligands $R_2P(R')_nPR_2$ (dppm: R = Ph, R′ = CH_2, $n = 1$; dppe: R = Ph, R′ = CH_2, $n = 2$; dppp: R = Ph, R′ = CH_2, $n = 3$; dppb: R = Ph, R′ = CH_2, $n = 4$; dppf: R = Ph, R′ = ferrocenyl, $n = 1$) with silver(I) methanesulfonate have been synthesized and characterized both in solution (^1H, ^{31}P NMR) and in the solid state (IR, single crystal X-ray structure analysis). The two different stoichiometries have been found to depend on the molar ratio of ligand to metal employed and the nature of the diphosphine ligand. In AgO_3SMe:dppp,dppb $(1:1)_2$, in the $[Ag(P^\wedge P)_2Ag]$ arrays, the silver atoms are also bridged by anion oxygen atoms, in disparate fashion commensurate with the different Ag···Ag distances.

1. Introduction

Silver methanesulfonate is photostable and commercially available, showing no air sensitivity, and employed as a standard for silver CP/MAS experiments [1]. Some reports have appeared recently on silver sulfonate derivatives exhibiting a rich structural diversity, as exemplified in one-, two- or three-dimensional polymeric structures [2–6]. However, the number of silver species thus far isolated stabilized by Lewis bases or other ancillary ligands is very limited, notwithstanding their potential use in catalysis [7] and in materials science [8], and the well-known versatility of methanesulfonate precursors, through, for example, the relative lability of bound RSO_3^- maintained throughout the d-block metal ions [9]. Organophosphine and phosphite stabilized silver(I) methanesulfonate complexes have been described recently [10], also discussing their thermal stability; syntheses, structures and luminescence of mononuclear, dinuclear and tetranuclear silver(I) sulfonate complexes with PPh_3 have also been reported [11]. Further it has recently been shown that the dinuclear, cyclic structural motif $[Ag_2(\text{diphosphine})_2]^{2+}$ can be employed as a synthon for building up coordination cages containing large cavities [12], depending on the chain between the two phosphorus donor sites. Here we report on the interaction between silver(I) methanesulfonate with diphosphine ligands, which, to date, have been neglected with respect to monodentate phosphines.

2. Experimental

2.1. Materials and methods

AgO_3SMe and $R_2P(R')_nPR_2$ (dppm: R = Ph, R′ = CH_2, $n = 1$; dppe: R = Ph, R′ = CH_2, $n = 2$; dppp: R = Ph, R′ = CH_2, $n = 3$; dppb: R = Ph, R′ = CH_2, $n = 4$; dppf: R = Ph, R′ = ferrocenyl, $n = 1$) were purchased from Aldrich and used without further purification. All reactions were carried out under an atmosphere of dry oxygen-free dinitrogen, using standard Schlenk techniques and protected from light. All solvents were dried, degassed and distilled prior to use. Elemental analyses (C,H,S) were performed with a Fisons Instruments 1108 CHNS-O Elemental Analyser. IR spectra were recorded from 4000 to 100 cm^{-1} with a Perkin–Elmer System 2000 FT-IR instrument. ^1H and ^{31}P NMR spectra were recorded on a VXR-300 Varian spectrometer operating at room temperature (300 MHz for ^1H) and on a Mercury-Plus Varian 400 NMR spectrometer (400 for ^1H and 162.4 MHz for ^{31}P, respectively). Referencing is relative to TMS (^1H) and H_3PO_4 (^{31}P). The electrical resistance of CH_2Cl_2 and acetone solutions was measured with a Crison CDTM 522 conductimeter at room temperature. Melting points were obtained using a Stuart SMP3 melting point apparatus and were not corrected. Positive and negative electrospray mass spectra were obtained with a Series 1100 MSI detector HP spectrometer, using an acetonitrile mobile phase. Solutions (3 mg/mL) for electrospray ionization mass spectrometry (ESI MS) were prepared using reagent grade acetone or acetonitrile. For the ESI MS data, masses and intensities were compared to those calculated by using the IsoPro Isotopic Abundance Simulator Version 2.1 [13]; peaks containing silver(I) and copper ions are identified as the centres of isotopic clusters.

---

* Corresponding author. Tel.: +39 0737 402234; fax: +39 0737 637345.
E-mail address: Claudio.pettinari@unicam.it (C. Pettinari).

0020-1693/$ - see front matter © 2009 Elsevier B.V. All rights reserved.
doi:10.1016/j.ica.2009.02.036

2.2. Syntheses

*2.2.1. Synthesis of AgO_3SMe:dppm (1:1) (**1**)*

AgO_3SMe (0.203 g, 1.0 mmol) was added to an ethanol solution (30 ml) of dppm (0.384 g, 1.0 mmol), at room temperature. After the addition, the solution was stirred for 24 h at room temperature in the dark. A colorless precipitate formed in 70% yield which was filtered off and washed with ethanol (10 ml). M.p. 298–302 °C. ^1H NMR ($CDCl_3$, 293 K): δ 2.60s (SO_3CH_3), 3.29s (2H, $P(CH_2)P$), 7.1–7.5m (40H, PC_6H_5). ^{31}P NMR ($CDCl_3$, 293 K): 8.4 br. ^{31}P NMR ($CDCl_3$, 223 K): 9.56m ($^1J(^{107}Ag–^{31}P)$: 489 Hz, ^2J(P–P): 160 Hz; $^3J(^{107}Ag–^{31}P$: −4.5 Hz; $^1J(^{107}Ag–^{31}P)$: 561 Hz, $^3J(^{107}Ag–^{31}P$: −5.2 Hz). Λ_m (CH_2Cl_2, conc. = 0.88 × 10^{-3} M): 16.5 Ω^{-1} cm^2 mol^{-1}. IR (cm^{-1}): 3040sh [ν(C–H)], 1445w, 1309m, 1226m, 1150m, 1137s, 616w, 547m, 513s, 481m, 470m, 439w, 421w, 339m. *Anal.* Calc. for $C_{26}H_{25}AgO_3P_2S$: C, 53.17; H, 4.29; S, 5.46. Found: C, 53.32; H, 4.33; S, 5.55%. ESI MS (+): 1019 [100] $[Ag_2Cl(dppm)_2]^+$.

*2.2.2. Synthesis of AgO_3SMe:dppe (1:1) (**2**)*

AgO_3SMe (0.203 g, 1.0 mmol) was added to an ethanol solution (30 ml) of dppp (0.396 g, 1.0 mmol), at room temperature. After the addition, the solution was stirred for 24 h at room temperature in the dark. A colorless precipitate formed which was filtered off and washed with ethanol (10 ml). Crystallization from ethanol gave complex **2** as a microcrystalline solid in 60% yield. M.p. 249–252 °C dec. ^1H NMR ($CDCl_3$, 293 K): δ 2.4br 2.65s (4H, $P(CH_2)_2P$ + 3H, SO_3CH_3), 7.2–7.5m (20H, PC_6H_5). ^{31}P NMR ($CDCl_3$, 223 K): 9.7 d br ($^1J(Ag–^{31}P)$: 440 Hz); 13.5 dd ($^1J(^{109}Ag–^{31}P)$: 695 Hz; $^1J(^{107}Ag–^{31}P)$: 604 Hz. IR (cm^{-1}): 3117w, 3050w [ν(C–H)], 1558w, 1523w, 1512w, 1478m, 1433m [ν(C···C)], 1231m, 118m, 1170m, 1155m, 1106m, 1095m, 101m, 552s, 509s, 485m, 473m, 447m. *Anal.* Calc. for $C_{27}H_{27}AgO_3P_2S$: C, 53.92; H, 4.53; S, 5.33. Found: C, 54.00; H, 4.56; N, 5.28%. ESI MS (+): 429 [100] $[(dppeO_2)+H]^+$; 860 [80] $[(dppeO_2)_2+H]^+$; 905 [40] $[Ag(dppe)_2]^+$, 1048 [5] $[Ag_2Cl(dppe)_2]^+$.

*2.2.3. Synthesis of AgO_3SMe:dppp (1:1) (**3**)*

AgO_3SMe (0.203 g, 1.0 mmol) was added to a methanol solution (30 ml) of dppp (0.410 g, 1.0 mmol), at 40 °C. After the addition, the solution was stirred for 24 h at room temperature in the dark. A colorless precipitate formed which was filtered off and washed with methanol (6 ml). Crystallization from methanol gave complex **3** as a microcrystalline solid in 40% yield. M.p. 300 °C dec. ^1H NMR ($CDCl_3$, 293 K): δ 2.0–2.4br (6H, $P(CH_2)_3P$), 2.91s (3H, SO_3CH_3), 7.2–7.5m (20H, PC_6H_5). ^{31}P NMR ($CDCl_3$, 293 K): 9.9 dd ($^1J(^{109}Ag–^{31}P)$: 577 Hz; $^1J(^{107}Ag–^{31}P)$: 501 Hz. IR (cm^{-1}): 3067w, 3041w [ν(C–H)], 1585w, 1571w [ν(C···C)], 1308m, 1215m, 1197m, 1181m, 1153m, 1097m, 1037m, 1027m, 696s, 617m, 549s, 522s, 508s, 476s, 446s, 433m, 387m, 353m, 339m, 325m, 314m, 302m, 288w, 276w, 260w, 247w, 230w, 225w, 213w. *Anal.* Calc. for $C_{28}H_{29}AgO_3P_2S$: C, 54.65; H, 4.75; S, 5.21. Found: C, 54.45; H, 4.96; N, 5.30%. ESI MS (+): 443 [100] $[(dpppO_2)+H]^+$; 888 [60] $[(dpppO_2)_2+H]^+$; 933 [20] $[Ag(dppp)_2]^+$, 1076 [15] $[Ag_2Cl(dppp)_2]^+$.

*2.2.4. Synthesis of AgO_3SMe:dppb (1:1) (**4**)*

AgO_3SMe (0.203 g, 1.0 mmol) was added to a methanol solution (30 ml) of dppb (0.423 g, 1.0 mmol), at 40 °C. After the addition, the solution was stirred for 24 h at room temperature in the dark. The solution was then stored at 5 °C. Colorless crystals (65%) slowly formed which were filtered off and washed with methanol (10 ml). M.p. 261 °C dec. ^1H NMR ($CDCl_3$, 293 K): δ 1.95s br, 2.56s (6H, $P(CH_2)_4P$), 2.26s (3H, SO_3CH_3), 7.2–7.6m (20H, PC_6H_5). ^{31}P NMR ($CDCl_3$, 293 K): 1.7 dd ($^1J(^{109}Ag–^{31}P)$: 539 Hz; $^1J(^{107}Ag–^{31}P)$: 466 Hz). Λ_m (CH_2Cl_2, conc. = 0.5 × 10^{-3} M): 12.0 Ω^{-1} cm^2 mol^{-1}. IR (cm^{-1}): 3057m [ν(C–H)], 1584w, 1573w [ν(C···C)], 1310m, 1278m, 1211m, 1186m, 1165s, 1146s, 1100m, 1070m, 792w, 764m, 742s, 694s, 664m, 617w, 551m, 522m, 508m, 485m, 477m, 450w, 412w, 377w, 342w, 278w, 255w, 227w, 206w. *Anal.* Calc. for $C_{29}H_{31}AgO_3P_2S$: C, 55.34; H, 4.96; S, 5.09. Found: C, 55.02; H, 5.19; N, 4.75%. ESI MS (+): 457 [100] $[(dppbO_2)+H]^+$; 916 [40] $[(dppbO_2)_2+H]^+$; 961 [10] $[Ag(dppp)_2]^+$, 1104 [25] $[Ag_2Cl(dppb)_2]^+$.

*2.2.5. Synthesis of AgO_3SMe:dppf (1:1) (**5**)*

Derivative **5** has been prepared in 65% yield, following the procedure reported for **2**, by using AgO_3SMe (0.203 g, 1.0 mmol) and dppf (0.554 g, 1.0 mmol), at 40 °C. M.p. 186 °C dec. ^1H NMR ($CDCl_3$, 293 K): δ 2.85s (3H, SO_3CH_3), 4.2–4.4m (8H, PFc_2P), 7.2–7.6m (20H, PC_6H_5). ^{31}P NMR ($CDCl_3$, 293 K): 2.1 dd ($^1J(^{109}Ag–^{31}P)$: 498 Hz; $^1J(^{107}Ag–^{31}P)$: 438 Hz). Λ_m (Acetone, conc. = 0.9 × 10^{-3} M): 19.0 Ω^{-1} cm^2 mol^{-1}. IR (cm^{-1}): 1584w, 1570w, 1558w [ν(C···C)], 1235m, 1166m, 1151m, 1097m, 893w, 835w, 765m, 744m, 723w, 706w, 698s, 661w, 650w, 634w, 600w, 583w, 576w, 568w, 550m, 538m, 514m, 496m, 483m, 466m, 427m, 399w, 375w, 363w, 352w, 327w, 314w, 304w, 284w, 279m, 254w, 247m, 228m, 224m, 213m. *Anal.* Calc. for $C_{35}H_{31}AgFeO_3P_2S$: C, 55.51; H, 4.13; S, 4.23. C, 55.86; H, 4.35; N, 4.03%. ESI MS (+): 189 [100] $[Ag(MeCN)2]^+$; 662 [20] $[Ag(dppf)]^+$; 865 [40] $[Ag_2(O_3SMe)(dppf)]^+$.

*2.2.6. Synthesis of AgO_3SMe:dppe 1:2 (**6**)*

AgO_3SMe (0.203 g, 1.0 mmol) was added to a methanol solution (30 ml) of dppe (0.795 g, 2.0 mmol), at 40 °C. After the addition, the solution was stirred for 24 h at room temperature in the dark. A colorless precipitate formed which was filtered off and washed with methanol (6 ml). Crystallization from methanol gave complex **6** as a microcrystalline solid in 70% yield. M.p. 138 °C dec. ^1H NMR ($CDCl_3$, 293 K): δ 2.15, 2.45 (11H, $P(CH_2)_2P$ + SO_3CH_3), 7.1–7.5m (40H, PC_6H_5). ^{31}P NMR ($CDCl_3$, 293 K): +6.1 ($^1J(^{109}Ag–^{31}P)$: 266 Hz; $^1J(^{107}Ag–^{31}P)$: 230 Hz). Λ_m (acetone, conc. = 0.9 × 10^{-3} M): 97.5 Ω^{-1} cm^2 mol^{-1}. IR (cm^{-1}): 3056m [ν(C–H)], 1653w, 1636w, 1584w, 1570w, 1559w, 1540w, 1506w [ν(C···C)], 1482m, 1434s, 1308m, 1214s, 1198s, 1181s, 1154s, 1096s, 1039s, 998m, 863w, 744s, 700s, 663s, 654s, 617m, 550s, 520s, 506s, 480s, 457m, 448m, 348m. *Anal.* Calc. for $C_{53}H_{51}AgO_3P_4S$: C, 63.67; H, 5.14; S, 3.21. Found: C, 64.12; H, 5.15; N, 3.07%. ESI MS (+): 905 [100] $[Ag(dppe)_2]^+$.

*2.2.7. Synthesis of AgO_3SMe:dppp (1:2) (**7**)*

AgO_3SMe (0.203 g, 1.0 mmol) was added to a methanol solution (30 ml) of dppp (0.818 g, 2.0 mmol), at 40 °C. After the addition, the solution was stirred for 24 h at room temperature in the dark. A colorless precipitate formed which was filtered off and washed with methanol (6 ml). Crystallization from methanol gave complex **7** as a microcrystalline solid in 60% yield. M.p. 174 °C dec. ^1H NMR ($CDCl_3$, 293 K): δ 1.83s br, 2.4t (12H, $P(CH_2)_3P$), 2.80s (3H, SO_3CH_3), 7.2–7.5m (40H, PC_6H_5). ^{31}P NMR ($CDCl_3$, 293 K): −4.7 dd ($^1J(^{109}Ag–^{31}P)$: 254 Hz; $^1J(^{107}Ag–^{31}P)$: 220 Hz. Λ_m (acetone, conc. = 0.96 × 10^{-3} M): 90.1 Ω^{-1} cm^2 mol^{-1}. IR (cm^{-1}): 3058m [ν(C–H)], 1654w, 1585w, 1570w, 1508w [ν(C···C)], 1482m, 1434s, 1214s, 1199m, 1181m, 1154m, 1096m, 1040s, 1026w, 998w, 693s, 650s, 616m, 551m, 510s, 483, 439m, 407m, 349w, 304w, 290w, 279w, 254w, 226w. *Anal.* Calc. for $C_{55}H_{55}AgO_3P_4S$: C, 64.27; H, 5.39; S, 3.12. Found: C, 64.32; H, 5.35; N, 3.03%.

*2.2.8. Synthesis of AgO_3SMe:dppb (1:2) (**8**)*

AgO_3SMe (0.203 g, 1.0 mmol) was added to a methanol solution (30 ml) of dppb (0.818 g, 2.0 mmol), at 40 °C. After the addition, the solution was stirred for 24 h at room temperature in the dark. A colorless precipitate formed which was filtered off and washed with methanol (6 ml). Crystallization from methanol gave complex **8** as a microcrystalline solid in 45% yield. M.p. 222 °C dec. ^1H NMR

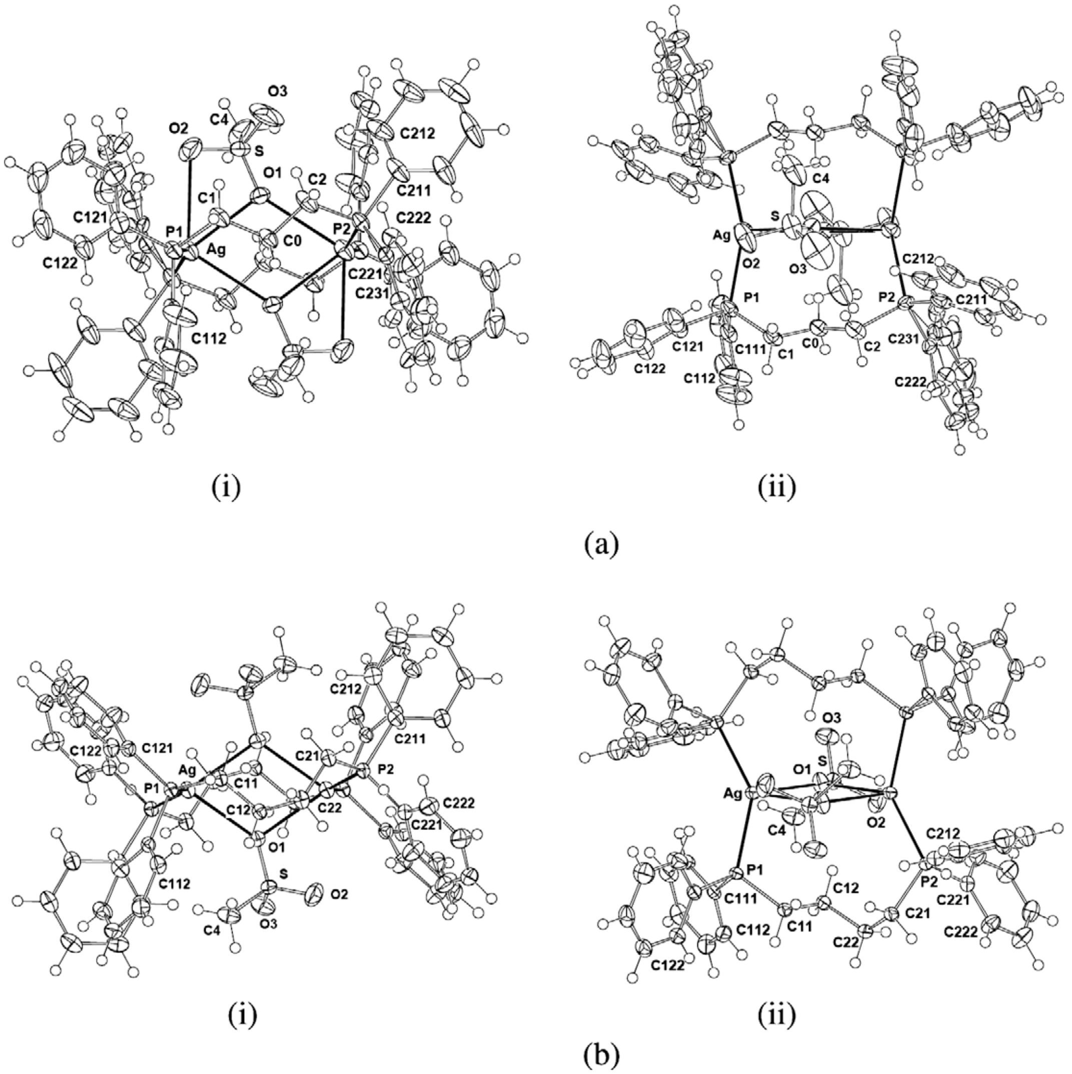

Fig. 1. (a, b) Projections of the dimers of **3**, **4**, (i, ii) through, and normal to, their Ag_2P_4 planes.

($CDCl_3$, 293 K): δ 2.05–2.23br (16H, P(CH_2)$_4$P), 2.73s (3H, SO_3CH_3), 7.1–7.45 m (40H, PC_6H_5). ^{31}P NMR ($CDCl_3$, 293 K): −0.1 dd ($^1J(^{109}Ag–^{31}P)$: 257 Hz; $^1J(^{107}Ag–^{31}P)$: 219 Hz. Λ_m (CH_2Cl_2, conc. = 0.5×10^{-3} M): 23.0 Ω^{-1} cm^2 mol^{-1}. IR (cm^{-1}): 3050m [ν(C–H)], 1585w, 1558w [ν(C···C)], 1216s, 1175s, 740s, 721m, 694sd, 618w, 550w, 518m, 479m, 444w, 396w, 344w, 301w. *Anal.* Calc. for $C_{57}H_{59}AgO_3P_4S$: C, 64.84; H, 5.63; S, 3.04. Found: C, 64.45; H, 5.65; S, 2.59%.

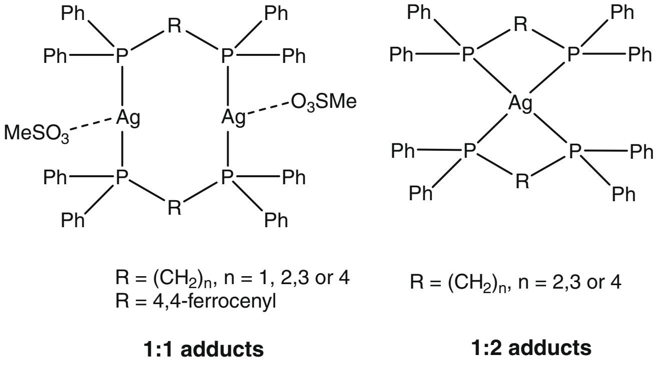

Chart 1.

2.3. Structure determinations

Full spheres of CCD area-detector diffractometer data were measured at ca. 153 K (monochromatic Mo Kα radiation, $\lambda = 0.7107_3$ Å; ω-scans, $2\theta_{max} = 58°$) yielding $N_{t(otal)}$ reflections, these merging to N independent (R_{int} cited), after 'empirical'/multiscan absorption correction (proprietary software), these being used in the full matrix least squares refinements on F^2, refining anisotropic displacement parameters for the non-hydrogen atoms, hydrogen atom treatment following a riding model; N_o reflections with $F > 4\sigma(F)$ were considered 'observed'. Neutral atom complex scattering factors were employed; computation used the SHELXL 97 program [14]. Reflection weights were $(\sigma^2(F^2) + (aP)^2 + bP)^{-1}$ $(P = (F_o^2 + 2F_c^2)/3)$. Pertinent results are given below and in the tables and Fig. 1, the latter showing 50% probability amplitude displacement envelopes for the non-hydrogen atoms, hydrogen atoms having arbitrary radii of 0.1 Å. Full *.cif* depositions reside with the Cambridge Crystallographic Data Centre, #708681,708682.

2.3.1. Crystal/refinement data

*2.3.1.1. AgO_3SMe:dppp (1:1)$_2$ (**3**).* $C_{56}H_{58}Ag_2O_6P_4S_2$, $M = 1230.8$. Triclinic, space group $P\bar{1}$ (C_i^1, No. 2), $a = 10.492(1)$, $b = 11.948(1)$ $c = 13.073(1)$ Å, $\alpha = 69.006(1)$, $\beta = 66.349(1)$, $\gamma = 66.857(1)°$, $V =$

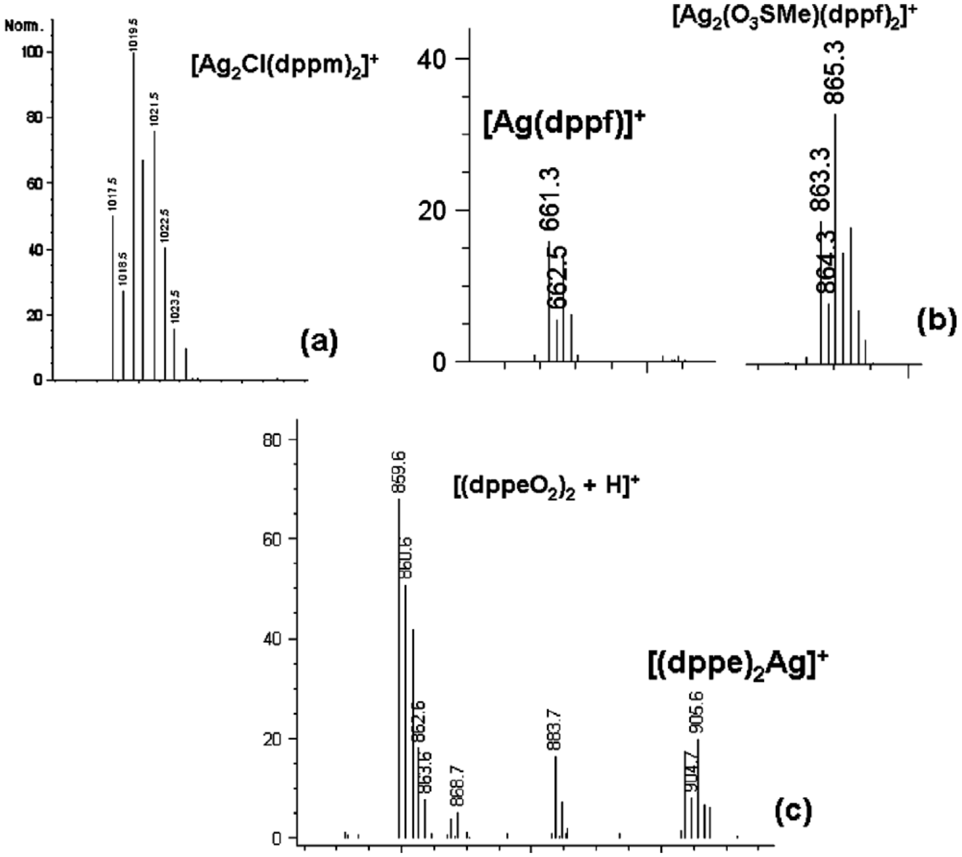

Fig. 2. ESI MS spectra (MeCN, positive mode) of compounds **1** (a), **5** (b) and **2** (c).

1341 Å^3. D_c ($Z = 1$) = 1.524 g cm^{-3}. μ_{Mo} = 0.98 mm^{-1}; specimen: 0.65 × 0.40 × 0.10 mm; '$T_{min/max}$ = 0.68. N_t = 15442, N = 6495 (R_{int} = 0.028), N_o = 5667; R_1 = 0.040, wR_2 = 0.108 (a = 0.056, b = 2.2); S = 1.05.

Variata. Phenyl ring 22n was modelled as disordered over two sites, occupancies refining to 0.644(7) and complement.

2.3.1.2. AgO$_3$SMe:dppb (1:1)$_2$, **4** *(·0.48H$_2$O).* $C_{58}H_{62}Ag_2O_6P_4S_2 \cdot 0.48H_2O$, M = 1267.5. Triclinic, space group $P\bar{1}$, a = 10.375(1), b = 12.010(1) c = 12.683(1) Å, α = 109.106(2), β = 91.682(2), γ = 109.104(2)°, V = 1395 Å^3. D_c ($Z = 1$) = 1.50$_9$ g cm^{-3}. μ_{Mo} = 0.94 mm^{-1}; specimen: 0.45 × 0.40 × 0.16 mm; '$T_{min/max}$ = 0.64. N_t = 15819, N = 6701 (R_{int} = 0.026), N_o = 6358; R_1 = 0.027, wR_2 = 0.076 (a = 0.045, b = 1.3); S = 1.05.

Variata. A difference map residue was modelled in terms of a water molecule oxygen fragment, O(01), occupancy refining to 0.228(8); associated hydrogen atoms were not located. O(01)···(sulfate) O(2) is 2.683(10) Å.

Table 1
Selected geometries, **3**.

Atoms	Parameter	Atoms	Parameter
Distances (Å)			
Ag–P(1)	2.4170(8)	S–O(1)	1.461(2)
Ag–P(2′)	2.3885(7)	S–O(2)	1.451(3)
Ag–O(1)	2.574(2)	S–O(3)	1.434(3)
Ag–O(1′)	2.866(2)	S–C(4)	1.772(5)
Ag–O(2)	2.890(4)	Ag···Ag′	4.4514(4)
Angles (°)			
P(1)–Ag–P(2′)	150.98(2)	Ag–O(1)–S	104.1(1)
P(1)–Ag–O(1)	99.22(5)	Ag–O(1′)–S′	146.2(1)
P(1)–Ag–O(1′)	97.22(5)	Ag–O(2)–S	90.9(2)
P(1)–Ag–O(2)	85.47(6)	O(1)–Ag–O(1′)	70.27(8)
P(2′)–Ag–O(1)	109.66(5)	O(1)–Ag–O(2)	51.75(7)
P(2′)–Ag–O(1′)	90.02(5)	O(1′)–Ag–O(2)	121.43(7)
P(2′)–Ag–O(2)	114.50(6)	Ag–O(1)–Ag	109.7(1)
P^P ligand torsions (°)			
Ag–P(1)–C(1)–C(0)	−57.5(2)	Ag–P(2)–C(2)–C(0)	51.3(2)
P(1)–C(1)–C(0)–C(2)	150.9(2)	P(2)–C(2)–C(0)–C(1)	−163.1(2)

Primed atoms are related by the intramolecular inversion centre.

3. Results and discussion

The diphosphine silver(I) methanesulfonate 1:1 adducts **1**–**5** were prepared by using equimolar quantities of the P^P-donor, in alcoholic solvents under nitrogen in moderate yield. By using a large excess of the diphosphine the 2:1 adducts **6**–**8** formed (Chart 1). The complexes were isolated as white solids. They are not sensitive to moisture and temperature, and insoluble in non-polar solvent like petroleum, whereas they are soluble in chlorinated solvents and acetone.

The IR spectra of all derivatives show a number of absorptions in the 1300–1000 cm^{-1} region, due to asymmetric and symmetric vibrations of SO$_2$ according to the literature and also a medium absorption at ca. 1030 cm^{-1} that can be assigned to the S–O vibration [15–17]. It is worth noting that the 1:1 adducts show a pattern of absorptions different to that found in the 2:1 species in which the O$_3$SMe is likely ionic. For example, in **3**, in which the sulfonate is covalently bonded, the symmetric absorption is found at ca. 1180 cm^{-1}, whereas in **6** in which an ionic O$_3$SMe is hypothesised, we have detected two strong absorptions between 1210 and 1190 cm^{-1}.

The conductivity values found for derivatives **1**–**5** in dichloromethane are higher than those found, for example, in analogous halide and pseudohalide derivatives [18] and are suggestive of a partial dissociation in solution. We cannot exclude the occurrence of equilibria such as Eq. (1), also taking into account that species analogous to $[Ag_2(\text{diphosphine})_2(O_3SMe)]^+$ [19] may be formed, but on the basis of NMR spectra (see below) we suggest in solution also the existence of the dissociation Eq. (2), so that both processes indicated here may be present.

$$[Ag_2(\text{diphosphine})_2(O_3SMe)_2] \leftrightarrows [Ag_2(\text{diphosphine})_2(O_3SMe)]^+ + [O_3SMe]^- \quad (1)$$

$$[Ag_2(\text{diphosphine})_2(O_3SMe)_2] \leftrightarrows [Ag(\text{diphosphine})_2](O_3SMe) + AgO_3SMe \quad (2)$$

Eq. (2) is consistent with the fact that dissolution of derivatives **2**–**4** in dichloromethane always yields small quantities of corresponding derivatives **6**–**8**.

The occurrence of the Eqs. (1) and (2) is also supported by the ESI MS spectra carried out in MeCN. In the positive mode, the spectra of **1**–**4** exhibit peaks due the cationic species $[Ag_2Cl(\text{diphosphine})_2]^+$ and $[Ag(\text{diphosphine})_2]^+$ consequent upon loss of methanesulfonate counter-ions (with exception of **1** in which the unique signal detectable is that due to $[Ag_2Cl(\text{dppm})_2]^+$ (Fig. 2a). However, no fragments containing two positive charges have been detected. In the ESI MS spectrum of **5** (positive mode) we have found signals due to both mononuclear $[Ag(\text{dppf})^+]$ and dinuclear $[Ag_2(O_3SMe)(\text{dppf})]^+$ (Fig. 2b and no signal due to 2:1:2 complex is present. In the spectra of the 1:2 adducts **6**–**8**, the unique signal detectable is that assignable to a $[Ag(\text{diphosphine})_2]^+$ species, confirming a greater stability of these species in solution. It is worth noting that addition of the corresponding diphosphine to solution of **2**–**4**, leads to an increase of the signals due to cationic $[Ag(\text{diphosphine})_2]^+$ species.

In the spectra of **2**–**4** also signals due to protonated oxidized diphosphines can be identified (see for example (Fig. 2c), whereas these signals are not present in the spectra of **6**–**8**. These results confirm at least the partial existence of the silver complexes **1**–**8** in solution, the 1:2 adducts **6**–**8** being, however, the most stable species with respect to the dinuclear adducts **1**–**4**. The negative electrospray spectra are always dominated by the presence of peaks due to $[O_3SMe]^-$, $[Ag(O_3SMe)_2]^-$ and also due to $[AgCl_2]^-$, (the Cl^- ion rising from the solvent).

^1H NMR spectra were recorded for all complexes and were consistent with the stoichiometries of the complexes. The CH_3 proton of O_3SMe falls in all complexes in the range 2.4–2.8 in accordance with the value previously reported [20]. The bridging methylene proton resonances in **1**–**7** appear as a broad singlet or multiplet between 1.8 and 2.60 ppm, shifted with respect to those found in the free donors and confirming the existence, at least partial, of the complexes in solution. The chemical shift of the methylene protons in **1** can be used for the evaluation of the charge changes on the coordinating P atoms. We have calculated the appropriate value on the basis of the empirical relation of Grim and Walton [21]

$$\delta_{CH_2}\ (\text{ppm}) = 1.57\sum q_i + 2.65 \quad (q_i = \text{charge on the } i\text{th phosphorus nucleus}).$$

The obtained change of charge, 0.20, correlates well with the upper frequency coordination shift in the ^{31}P NMR spectrum of **1**.

^{31}P chemical shifts ($CDCl_3$ solution) and ^{31}P–Ag coupling constants for derivatives **1**–**8**, are reported in Section 2. The room temperature ^{31}P NMR spectra of the complexes consists generally of unresolved broad doublets or multiplets. At low temperature (218–223 K), two resolved pairs of doublets, arising from coupling between the phosphorus and silver atoms, are observed in the accessible temperature range. In particular, in the spectra of derivatives **2**–**7** typical pairs of doublets, due to $^{131}J(^{31}P-^{107}Ag)$ and $^1J(^{31}P-^{109}Ag)$ coupling, are resolved at 218 K and the observed $^1J(^{107}Ag)/^1J(^{109}Ag)$ ratio is in good agreement with that calculated from the gyromagnetic ratio of the Ag nuclei [22]. The signal due to each free phosphine is always up-field with respect to that of the corresponding silver(I) complex. It has been suggested [23,24] that the spin–spin constant (J) between phosphorus and silver changes, depending on the number of coordinated phosphorus atoms in the silver complex, and that it is possible to determine the number of the latter from measurement of the J values in the ^{31}P NMR spectra. On this basis we hypothesised a AgP_2O_2 environment for **2**–**5** and AgP_4 for **6**–**8** in solution. The low temperature ^{31}P spectra of the 1:1 species consist often of a sharper double doublet, flanked by a less intense double doublet, characterized by similar coupling constants, that can be ascribed to the existence of two forms of the same species in solution and a second double doublet that increases with the time analogous to that found in the spectra of the 1:2 adducts **6**–**8** and that confirms the relevance of Eq. (2). A double triplet and a broad signal have been found at room temperature in the spectrum of **1** whereas the low temperature ^{31}P spectrum consists of an AA′XX′AA′ pattern [25] due to the non-equivalence of the phosphorus atoms (as emerges also from the X-ray data) and resulting from the large $^2J(P-P)$, for the three possible combinations of the two silver isotopes. The same pattern, has been found by us also for other known $[Ag_2(\text{dppm})_2(X)_2]$ species, supporting a binuclear structure for **1** [26]. We have calculated the values of the coupling constants from the NMR spectral data recorded at 223 K by applying the equations reported by van der Ploeg and van Koten [27].

Single crystal X-ray structure determinations of **3** and **4** show similar binuclear forms (Fig. 1, Tables 1 and 2), exhibiting the familiar [Ag(P^P)$_2$Ag] binuclear unit, with the silver atoms further bridged in these examples by a pair of sulfonate ligands. The Ag···Ag distances differ (4.0614(3); 4.4512(4) Å, in keeping with the increased n in the $(CH_2)_n$ bridges of the P^P ligands, despite the constraint of the bridging sulfonate groups. The latter are essentially symmetrically μ-OSO_2CH_3 bridging (Ag–O(1,1′) 2.496(2), 2.509(2); Ag···O(2′) 3.109(3) Å) in **4** (Table 2), less symmetrical 2.574(2), 2.866(2) Å with invasive Ag···O(2) interaction (2.890(4) Å), impacting on the remainder of the coordination environment of the silver atom in **3** (Table 1). Interestingly, despite the lack of close Ag···O(2) interaction in **4**, the symmetrical bridging interactions of O(1) may be considered sufficiently invasive to diminish the P–Ag–P angle from 150.98(2) in **3** to 139.63(2)°, both in turn considerably diminished relative to the value found in $AgClO_4$:dppp $(1:1)_2$ where, despite the feebly coordinating nature of the anion, there still is a pronounced anionic bridging interaction

Table 2
Selected geometries, **4**.

Atoms	Parameter	Atoms	Parameter
Distances (Å)			
Ag–P(1)	2.4316(5)	S–O(1)	1.464(2)
Ag–P(2′)	2.4175(5)	S–O(2)	1.451(2)
Ag–O(1)	2.496(2)	S–O(3)	1.446(2)
Ag–O(1′)	2.509(2)	S–C(4)	1.772(2)
Ag–O(2′)	3.109(3)	Ag···Ag′	4.0617(4)
Angles (°)			
P(1)–Ag–P(2′)	139.63(2)	Ag–O(1)–S	139.34(9)
P(1)–Ag–O(1)	105.77(4)	Ag–O(1′)–S′	111.28(8)
P(1)–Ag–O(1′)	93.04(5)	O(1)–Ag–O(1′)	71.48(5)
P(2′)–Ag–O(1)	97.25(4)	Ag–O(1)–Ag′	108.52(5)
P(2′)–Ag–O(1′)	125.97(4)		
P^P ligand torsions (°)			
Ag–P(1)–C(11)–C(12)	−57.2(1)	Ag–P(2)–C(21)–C(22)	66.5(2)
P(1)–C(11)–C(12)–C(22)	176.4(1)	P(2)–C(21)–C(22)–C(12)	−75.4(2)
C(11)–C(12)–C(22)–C(21)	−74.0(2)		

Primed atoms are related by the intramolecular inversion centre.

with (in two phases) P–Ag–P 157.40(2)–160.53(2)° with Ag–P 2.3914(4)–2.405(2) and Ag···Ag 4.7254(3)–4.878(2) Å [18].

References

[1] G.H. Penner, W. Li, Solid State Magn. Res. 23 (2003) 168.

[2] G. Smith, B.A. Clouth, D.E. Lynch, K.A. Byriel, C.H.L. Kennard, Inorg. Chem. 37 (1998) 3236.

[3] M. Bardaji, O. Crespo, A. Laguna, A.K. Fischer, Inorg. Chim. Acta 304 (2000) 7.

[4] H.-Y. Liu, H. Wu, J.-F. Mia, S.-Y. Song, J. Yang, Y.-Y. Liu, Z.-M. Shu, Inorg. Chem. 46 (2007) 7299.

[5] G.K.H. Shimizu, G.D. Enright, C.I. Ratcliffe, K.F. Preston, J.L. Reid, J.A. Ripmeester, Chem. Commun. (1999) 1485.

[6] P.F. Charbonnier, R.F.H. Loiseleur, Acta Crystallogr., Sect. B 37 (1981) 822.

[7] F. Colombo, R. Annunziata, M. Benaglia, Tetrahedron Lett. 48 (2007) 2687.

[8] K. Ozawa, F. Iso, Y. Nakao, Z.X. Cheng, H. Fujii, M. Hase, H. Yamaguchi, J. Eur. Ceram. Soc. 27 (2007) 2665.

[9] G.A. Lawrance, Chem. Rev. 86 (1986).

[10] Y.-Y. Zhang, Y. Wang, X. Tao, N. Wang, Y.-Z. Shen, Polyhedron 27 (2008) 2501.

[11] F.-F. Li, J.-F. Ma, Y. Yang, H.-Q. Jia, N.-H. Hu, J. Mol. Struct. 787 (2006) 106.

[12] P.W. Miller, M. Nieuwenhuyzen, J.P.H. Charmant, S.L. James, Inorg. Chem. 47 (2008) 8367.

[13] M.W. Senko, IsoPro Isotopic Abundance Simulator, vol. 2.1, National High Magnetic Field Laboratory, Los Alamos National Laboratory, Los Alamos, NM.

[14] G.M. Sheldrick. SHELXL 97, A Program for Crystal Structure Refinement, University of Göttingen, 1997.

[15] M.G. Miles, G. Doyle, R.P. Cooney, R.S. Tobis, Spectrochim. Acta A 25 (1960) 1515.

[16] R. Bala, R.P. Sharma, A.D. Bond, J. Mol. Struct. 830 (2007) 198.

[17] C.Y. Panicker, H.T. Varghese, D. Philip, H.I.S. Nogueira, Spectrochim. Acta A 64 (2006) 744.

[18] Effendy, C. di Nicola, M. Fianchini, C. Pettinari, B.W. Skelton, N. Somers, A.H. White, Inorg. Chim. Acta 358 (2005) 763.

[19] P. Teo, L.L. Koh, T.S.A. Hor, Inorg. Chem. 47 (2008) 9561.

[20] D.A. Edwards, R.M. Harker, M.F. Mahon, K.C. Molloy, J. Mater. Chem. 9 (1999) 1771.

[21] S.O. Grim, E.D. Walton, Inorg. Chem. 19 (1980) 1982.

[22] J. Goodfellow, Post-transition metals, copper to mercury, in: J. Mason (Ed.), Multinuclear NMR, Plenum Press, New York, 1987, pp. 563–589 (Chapter 21).

[23] E.L. Muetterties, C.W. Alegranti, J. Am. Chem. Soc. 94 (1972) 6386.

[24] R.G. Goel, P. Pilon, Inorg. Chem. 17 (1978) 2876.

[25] Z. Yuan, N.H. Dryden, J.J. Vittal, R.J. Puddephatt, Can. J. Chem. 72 (1994) 1605.

[26] Effendy, J.V. Hanna, F. Marchetti, D. Martini, C. Pettinari, R. Pettinari, B.W. Skelton, A.H. White, Inorg. Chim. Acta 357 (2004) 1523.

[27] A.F.M.J. van der Ploeg, G. van Koten, Inorg. Chim. Acta 51 (1981) 225.